Cement and Concrete Research 40 (2010) 1138–1147

Contents lists available at ScienceDirect

Cement and Concrete Research

journal homepage: http://ees.elsevier.com/CEMCON/default.asp

A volumetric technique for measuring the coefficient of thermal expansion of hardening cement paste and mortar

Roman Loser, Beat Münch, Pietro Lura *

Empa, Swiss Federal Laboratories for Materials Testing and Research, Switzerland

ARTICLE INFO

Article history:
Received 3 December 2009
Accepted 22 March 2010

Keywords:
Thermal expansion coefficient
Fresh concrete (A)
Hydration (A)
Shrinkage (C)

ABSTRACT

Knowledge of the coefficient of thermal expansion (CTE) is of paramount importance for the determination of the cracking risk of concrete structures at early ages. This paper presents a novel technique which is suitable to measure the CTE of hardening materials with high accuracy starting from casting time.
The technique consists of casting a small amount of cement paste or mortar into flexible membranes. The specimens are immersed in an oil bath, whose temperature is rapidly changed and then kept constant in repeating cycles. By suspending the sample from a high-precision balance and reading the change of mass after each temperature step, the CTE is calculated with high accuracy from the measured temperature and strain.
Results on cement pastes and mortars (water/cement 0.3) showed a good repeatability. In particular, a sudden decrease in the CTE at setting time, followed by a gradual increase as the cement paste self-desiccates, was measured.

1. Introduction

Volumetric deformations of cement paste at early ages may produce both microcracking at the paste–aggregate interface [1,2] and macrocracking of a concrete structure due to external restraint [3–6]. These deformations are caused by changes in the moisture state and in the temperature of the concrete. Temperature changes may be induced by the heat release associated with the hydration of cement [7], by changes in ambient temperature and by cooling due to evaporation [8]. While moisture and temperature effects can be studied separately in the laboratory, at the construction site they occur simultaneously and their interaction may increase the early-age cracking risk of concrete structures.

Attempts at separating thermal- and moisture-related deformations are often based on assumptions of decoupling [9–12] and on a constant thermal expansion coefficient (CTE) [13,14]. Albeit convenient in numerical calculations, these assumptions are far from reality. In fact, on the one hand, moisture-related deformations (i.e., autogenous and drying shrinkage) are temperature-dependent [5,15,16]. On the other hand, the CTE of hardened concrete changes with the progress of hydration and with the moisture level of the cement paste [17,18]. In addition, delayed deformations due to moisture redistribution after a temperature step have also been observed in cement pastes [19].

A review of different methods for measuring CTE of cementitious materials was written by Boulay [20], while De Schutter [21] compared CTE measurements at early age from different sources. Measurements of CTE at early age have been mostly carried out by monitoring the linear length change of a specimen subjected to temperature cycles. The length change was measured, e.g., with LVDTs [9,22,23], comparators, lasers [24,25], embedded extensometers [26], cast-in vibrating wire extensometers [27] and fiber-optic deformation sensors [11]. Even if it is possible with some techniques to start the measurements before setting (e.g. [9,22,25,27]), a length change is not clearly defined for a material that is still fluid. Moreover, cast-in measuring points (e.g. [9,22,23]) are not yet firmly anchored in concrete before and around setting time, nor is the bond between concrete and a vibrating wire extensometer [27] fully developed. Measurements of CTE at early ages with embedded extensometers, when the elastic modulus of the concrete is low, will also be influenced by the stiffness of the sensor [28]. For these reasons, CTE results before and around setting obtained with linear methods should be considered with caution. The general trend of these measurements is however that the CTE of concrete rapidly decreases around setting time [9,10,22,24,25,27]. After setting, CTE results of hardened concrete at early ages appear contradictory, with mixtures showing either an increase [9,29], a constant value [11,25] or for some mixture also a decrease of CTE with maturity or degree of hydration [11]. Moreover, the measurements usually show a large scatter [23,25]. It is believed that at least a part of these contradictory results arises from artifacts of the measurement techniques used. In fact, since during hydration a cement paste is transitioning from a fluid to a solid, length change measurements are incapable of capturing the bulk volume changes induced in a fluid. Therefore, a volume-based technique may be needed to resolve these contradictions.

Loukili et al. [30] measured the CTE of a low water/cement (w/c) mortar using a volumetric method. Samples of mortars, weighing 300–400 g, were enclosed in a latex membrane and immersed in a water bath

* Corresponding author.
E-mail address: pietro.lura@empa.ch (P. Lura).

0008-8846/$ – see front matter © 2010 Elsevier Ltd. All rights reserved.
doi:10.1016/j.cemconres.2010.03.021

while suspended from a balance. The CTE was measured immediately after batching every hour in the first 6 h after mixing. For each measurement, the temperature of the bath was increased by 10 °C during 10 min. From the change in submerged weight of the sample, the CTE was derived. The CTE changed from about 90 µm/m/°C to about 15 µm/m/°C after setting. According to the authors, the measurement device is not sensitive enough to measure the low CTE values; for this reason, no measurement after 6 h is reported. In a later study by the same research group, Turkry et al. [31] measured the volumetric CTE of a low w/c cement paste in the first 24 h at 20 and 30 °C on cement paste samples weighing about 90 g. Every hour, the bath temperature was increased by 4 °C within a period of about 7 min and then immediately decreased to the isothermal temperature. From the change in submerged weight of the sample, the CTE was derived. The measured CTE changed from about 150 µm/m/°C in the first hours to about 30 µm/m/°C after setting; however, the scatter was large, with single measurements ranging from 10 to 40 µm/m/°C after setting. An observation about these studies [30,31] is that the rather large samples and the short temperature cycles probably did not allow reaching thermal equilibrium within each cycle. In addition, the use of a latex membrane in a water bath probably lead to water penetration into the samples, which would alter the moisture state of the sample besides influencing the readings of the balance [32,33].

The technique for measuring CTE proposed in this study is based on a recently-developed method for assessing autogenous deformation in cement-based materials [33,34]. It consists of casting very small amounts (25–30 g) of cement pastes or mortars into flexible polyisoprene membranes. The specimens are then immersed in a silicone oil bath and suspended from a high-precision balance. The temperature of the buoyancy fluid can be precisely regulated and rapidly changed. By changing the temperature of the water bath, the cementitious sample can be subjected to repeated temperature cycles of desired amplitude. The temperature is changed stepwise and held constant after each temperature step to reach temperature equilibrium. At this point, the CTE can be calculated with great accuracy from the measured temperature and strain.

It is pointed out that the technique developed here could be adapted to study the evolution in the thermal dilation coefficient in other hardening materials, for example various types of thermoplastics [35,36] and in particular epoxy resins [37] or glass ionomer cements used as restorative materials for tooth implants [38].

2. Materials

2.1. Materials

Four different hardening and non-hardening materials were used in the CTE measurements. As hardening materials, a cement paste and a mortar containing 41% by volume of well rounded sand were used. The sand was composed of dense sandstone, limestone and igneous rock, with absorption of less than 1% and maximum grain size of 1.0 mm. In both cases, the binder was an ordinary Portland cement (OPC). The w/c was 0.30 for paste and mortar. Workability was controlled by using a polycarboxylate-type superplastizicer (SP) with different amounts for paste and mortar. The aim was to have an acceptable flow behavior for filling the elastic membrane without any air voids. At the same time, bleeding needed to be minimized [33].

The non-hardening materials were a paste containing limestone powder (LP) and water with a water-to-powder-ratio (w/p) of 0.30 by mass as well as pure deionised water. No SP was necessary for the LP paste as the workability was already in the expected range. An overview over the different mixtures used is given in Table 1.

Setting of the cement paste was determined by Vicat needle following the procedure described in standard EN 196-3. The mixture proportioning was according to Table 1 and the Vicat ring was covered with a thin rubber foam that prevented evaporation but did not hinder penetration of the needle into the paste. Initial setting occurred at 5.7 h and final setting at 6.9 h.

Table 1
Mix composition. SP = superplastizicer; LP = limestone powder.

Type	Water [kg/m^3]	Cement or limestone [kg/m^3]	Sand [kg/m^3]	SP [kg/m^3]
Cement paste	480	1615	–	6.5
Mortar	274	940	1097	14.1
LP paste	453	1510	–	–
Water	1000	–	–	–

2.2. Sample preparation

The deionised water used for all mixtures was boiled in a water cooker for about 15 s in order to prevent the forming of air bubbles during temperature cycles. Air bubbles may constitute a source of error in volumetric measurements [33], especially in measurements involving a temperature change. The water was cooled down to ambient temperature (20 °C) before mixing. Pastes and mortar were mixed in a vacuum mixer (Twister evolution 1822-0000) for 2 min at 450 rpm. The mixer had a maximum volume of 500 ml and was filled with about 100 ml during mixing.

As elastic membrane, commercially-available condoms made of polyisoprene (Durex Avanti Ultima) were used. The condom was unrolled and the lubricant was carefully removed with a paper towel. Subsequently, the condom was attached to a plastic ring, which was fixed to a column (Fig. 1, left). After filling the condom with about 150 g of the mixture, the condom was pulled through a metallic clamp with a thin string and the clamp was squeezed with a pincer. Attention was paid to avoid entrapment of air bubbles and harming the condom. The string (0.35-mm mono-filament PTFE/silicone string, fishing line) was fixed with a knot and the excess part of the condom was cut off. The weight of the sample including part of the condom (0.39 g), clamp (0.69 g) and string (0.05 g) was between 26 g and 30 g for cement paste, mortar and limestone paste and about 16 g for the sample with water. A view of the sample ready for measurement is shown in Fig. 1, right.

3. Methods

3.1. Conceptual description of the method

The CTE was determined using Archimedes' principle. The test sample was filled in an elastic membrane (condom) and hung from a balance in a temperature-controlled buoyancy liquid. The volume of the sample V_s at temperature T was calculated as follows:

$$V_s(T) = \frac{m_{s,A} - m_{s,L}(T)}{\rho_L(T)} \quad (1)$$

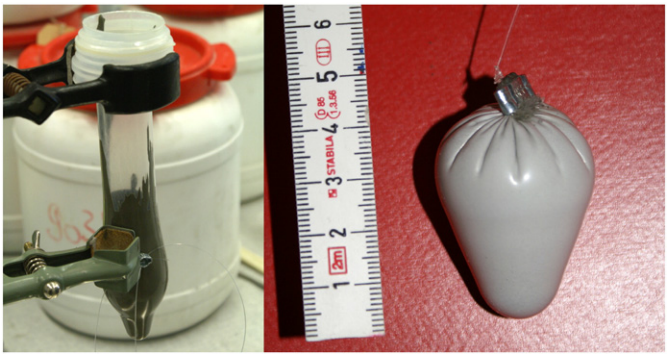

Fig. 1. Left: condom filled with cement paste fixed to a plastic ring, clamp and string during the filling procedure. Right: sample of cement paste ready for measurement.

where $m_{s,A}$ is the mass of the sample measured in air, $m_{s,L}(T)$ the mass of the sample in the buoyancy liquid and $\rho_L(T)$ the density of the buoyancy liquid at temperature T.

As the temperature of the buoyancy liquid changed and with it the temperature in the sample, the volume of the sample changed as well. The resulting difference in buoyancy was measured by the balance as a change in mass; however, the change in mass also depended on the density change of the buoyancy liquid. As a consequence, to calculate the volume change ΔV_s from the mass change when changing the temperature from T_1 to T_2, the temperature dependence of the buoyancy liquid, $\rho_L(T)$, needed to be known:

$$\Delta V_s(T_1,T_2) = V_s(T_1) - V_s(T_2) = \frac{m_{s,A} - m_{s,L}(T_1)}{\rho_L(T_1)} - \frac{m_{s,A} - m_{s,L}(T_2)}{\rho_L(T_2)}. \quad (2)$$

From the volume change, the volumetric CTE β_T was calculated according to Eq. (3):

$$\beta_T = \frac{\Delta V_s(T_1,T_2)}{V_s(T_1)\cdot(T_1 - T_2)}. \quad (3)$$

Assuming an exactly isotropic behavior of the material, the linear CTE α_T could be approximated as follows:

$$\alpha_T \approx \frac{\beta_T}{3}. \quad (4)$$

By changing the temperature in the bath periodically, it was possible to determine the evolution of the CTE as a function of time.

Different factors may influence the accuracy of the described method for the determination of CTE. The most important of these are discussed in detail in the following section.

3.2. General comments about buoyancy fluid, temperature regulation and sample size

Previous work on autogenous deformation of cement paste [33] showed that samples enclosed in an elastic membrane and immersed in a water bath absorbed a significant amount of water. Different types of membranes, e.g. latex and polyurethane condoms, proved to be all permeable in these conditions. This water absorption started upon immersion of the sample in the bath and continued at least for several weeks [33]. Water absorption changed the weight of the immersed samples, thereby introducing a significant error in the autogenous deformation measurement [33]. Moreover, water absorption from the bath changed the moisture state of the samples, which could not be considered sealed anymore.

As the CTE of cementitious materials depends on their moisture state [17,18], water was used in this research as buoyancy liquid only in one measurement, to allow for comparison to other liquids. All other measurements were performed in an oil bath. Lura and Jensen [33] showed that in samples enclosed by polyurethane membranes immersed in paraffin oil, a negligible amount of paraffin oil was absorbed into the sample during a few days of immersion at constant temperature. In the present study, rapid changes of the temperature of the sample were necessary to measure the CTE at a given point in time. For this reason, it seemed opportune to use as a buoyancy liquid the same liquid circulating in the temperature bath, so that the liquid circulating in the bath would be in immediate contact with the sample. Given these limitations, the choice fell on silicone oil (polydimethylsiloxane).

The density change of a liquid as a function of temperature is substantially higher than for a solid. The silicone oil used in this study has a volumetric CTE of about $1200 \cdot 10^{-6}$/°C at 20 °C [39], water of $207 \cdot 10^{-6}$/°C [40], while the volumetric CTE of hardened cement paste is estimated to be around 30 to $75 \cdot 10^{-6}$/°C, corresponding to a linear CTE of 10 to 25 µm/m/°C [17,18,41,42]. Since CTE of the buoyancy liquid is about 16 to 40 times higher than the one of the immersed material, both the temperature-dependent density change of the oil and the oil temperature at the beginning and at the end of the temperature step needed to be known with high precision and compensated for. For the same reason, the temperature at the end of the temperature step had to be kept constant without any considerable cycling around the target temperature. Otherwise, the mass measurement would scatter in a range, which would represent a considerable part of the apparent mass change produced by the volume change of the cement paste. However, every thermostat shows a certain cycling of the temperature around the target value, which depends on the pump force for circulating the liquid and on the nature of the liquid. For the setup used in this study, the temperature of the bath oscillated in the range of ±0.2 °C for the used thermostat at mid-range pump force and with silicone oil as fluid. The higher the pump force, the lower the cycling of the temperature but the higher the influence on weight measurement due to increased movement of the sample.

A possible solution for this problem is to dampen the temperature oscillations by suspending the sample in a closed container separated from the main bath liquid. The container could be of a material of high heat conductivity (e.g. copper) to facilitate a rapid temperature change during the imposed temperature steps. This option was explored in the first phase of the development of the measuring technique. However, the temperature change in the closed container was very slow compared to the change of the surrounding fluid and, moreover, the final temperature in the container was not uniform over the height due to the absence of turbulence in the liquid. A compromise between fast temperature regulation and constant temperature within the temperature steps was finally reached by using a meshed container, whose openings were optimized until the temperature change was fast enough and the temperature in the container almost constant and uniform over the height.

Another important point is the dimension of the sample. For a large sample size, the measured mass change due to volume change is larger, with a positive effect on the accuracy of the mass measurement. At the same time, the larger the sample, the longer it takes to reach a temperature equilibrium with the surrounding fluid; this is a problem both during the imposed temperature steps and also when heat is released by the hydration reactions. Therefore, it is convenient to limit the dimensions of the sample while employing a high-precision balance.

3.3. Detailed description of the setup

During the measurements, the samples hung from a hook beneath the balance plate. The balance was a Mettler-Toledo AB 304-S/FACT, with sensitivity 0.1 mg for weights between 0 and 320 g. The measuring accuracy determined for this specific balance was 0.28 mg for a weight of 32 g, corresponding approximately to the weight of the samples. A maximum difference of 0.1 mg, equal to the sensitivity of the balance, was determined with repeated measurements on the same sample. This results in a nominal repeatability of the measured strain of about 2–3 µm/m, considering typical sample weights of 25–30 g, silicone oil as buoyancy liquid, and isotropic deformations. The actual uncertainty on the measured strain is much higher, being dominated by a number of factors, including density change of the oil, temperature oscillations and possibly drift of the balance in time. The balance was placed on a concrete table to minimize vibrations. The table was provided with a 60-mm circular hole through which the string passed. A view of the test setup is shown in Fig. 2, left.

The sample itself was submerged in silicone oil (polydimethylsiloxane), which was tempered by using a thermostat (RE312, Lauda Ecoline Staredition) with a container of dimensions $200 \times 200 \times 200$ mm^3. Most of the surface of the bath was covered with a lid to reduce heat loss and thermal gradients. Oil circulation in the bath, which helped keeping the sample temperature constant, was enabled by an adjustable pump in the thermostat. Temperature in the bath was measured and controlled

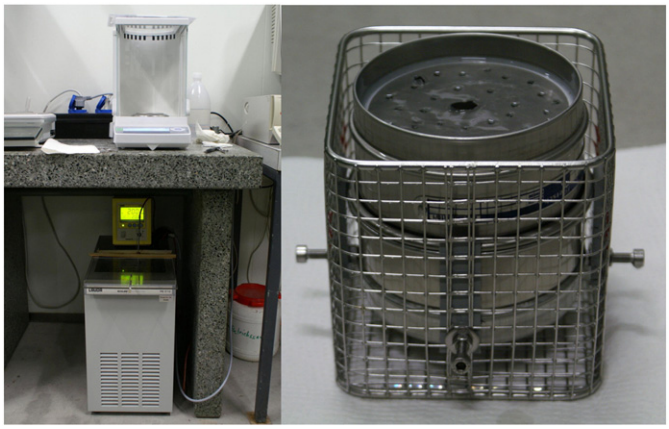

Fig. 2. Left: test setup with balance and thermostat. Right: permeable box, complete with upper removable and lower fixed sieve with holes for rapid circulation of the buoyancy liquid and permeable basket for fixation of the sieves.

by a temperature sensor PT 100-94 with a measuring accuracy of 0.02 K (sensitivity 0.01 K). With the thermostat, it was possible to program cycles of different temperature steps and duration.

In the oil bath, the sample was surrounded by a permeable box, consisting of two stainless steel sieves (Fig. 2, right) with sieve gaps of 63 µm which were fixed together in a basket built of mesh wire. The upper sieve with the hole for the string could be removed for insertion of the sample into the box. The lower sieve was permanently fixed to the basket and was lifted off from the bottom of the bath for better oil circulation. The gaps in the sieve were found to be too small to enable fast temperature adaptation in the box. Therefore, both the upper and the lower sieves were additionally perforated with holes of 4 mm in diameter. The number of perforations was increased until an optimum between fast temperature adaptation and temperature stability was reached within the permeable box. This was controlled by a temperature sensor placed in the middle of the two sieves. The example at set temperature of 23.0 °C in Fig. 3 shows the situation with the final perforation. While the temperature in the surrounding bath oscillates between 22.91 °C and 23.12 °C, the temperature in the box oscillates only between 22.95 °C and 22.99 °C under constant conditions (last half hour of the temperature cycle, see Section 3.4). Additionally, the temperature profile in the box was measured from the bottom to the top. The temperature was uniform in the centre of the box, from about 10 mm from each end of the sieves. Therefore, attention was paid to place the sample in the middle of the permeable box during the measurements.

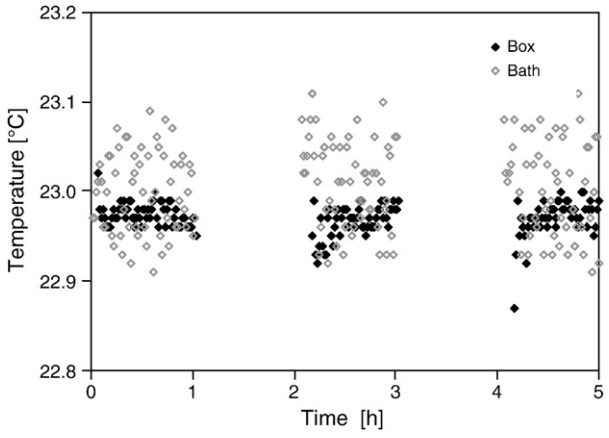

Fig. 3. Temperature measured in the permeable box and the surrounding bath at set temperature of 23.0 °C.

Since the accuracy of the oil temperature is the main influencing parameter on the results, an additional temperature sensor (PT 100-94) was placed directly beside the sample inside the box. The temperature beside the sample was measured and recorded automatically at regular intervals by the controlling software.

3.4. Measurement procedure

The immersed weight of the sample was measured and recorded automatically at the same intervals as the temperature beside the sample. Measurements were generally recorded every minute from 20 min after mixing up to a maximum of 120 h. In all graphs the time was zeroed at mixing time.

The temperature in the bath was changed in cycles of 60 or 90 min and with different temperature steps. This range was chosen because a temperature measurement in a sample of about 35 g by means of a thermocouple showed that the temperature change in the sample is strongly delayed compared to the bath temperature. While for a temperature step of 6 °C it took about 8 min to reach complete temperature equilibrium of the buoyancy liquid in the perforated box, the temperature in the sample was completely equilibrated after 28 min only (Fig. 4, left). A maximum temperature increase of 0.6 °C was measured in the centre of the sample due to hydration heat (Fig. 4, right). The temperature increase started about 6 h after mixing, while the temperature peak was reached after 13–14 h. After about 25 h the temperature was equilibrated again.

A typical plot of the immersed mass when temperature is changed periodically every 60 min from 23 °C to 17 °C and back is shown in Fig. 5. The sample is a cement paste according to Table 1.

The general increase in mass at the beginning is due to autogenous shrinkage of the cement paste. Moreover, the upper and lower envelope curves are the result of the cyclic temperature change in the buoyancy liquid. Having a closer look at the mass steps (Fig. 6) it can be recognized that the mass is decreasing with decreasing temperature. However, the opposite would be expected when only the volume of the cement paste was decreasing with temperature. Since the density of the oil is increasing when temperature decreases, this means that the effect of the increase in the buoyancy force is dominating the decreasing volume of the cement paste, leading to the observed decrease in mass. As shown in Fig. 4, the temperature in the cement paste lags behind the temperature of the oil and as a result also the volume change is delayed. This is the reason why, in Fig. 6, a small back drift in the recorded mass can be observed after the large mass change due to the change of the buoyancy in the liquid. As the temperature of the liquid is precisely measured with the temperature sensor placed near the sample in the buoyancy liquid, the time- and temperature-dependent volume of the cement paste can be calculated using Eq. (1). For this purpose, the temperature-dependent density of the oil has to be known.

3.5. Determination of the oil density

Since the temperature-dependent density of the oil is crucial for the accurate determination of the CTE of the cement paste, the average temperature-dependent density change of silicone oil given by the producer [39] was not found accurate enough for the aim of this study. Therefore, the temperature-dependent density change of the specific oil used in the bath had to be determined in advance. This was made by submerging samples with known CTE into the oil and measuring temperature-dependent mass change with the balance. From the mass change and the volume of the sample, calculated with the known CTE, the density of the oil at different temperatures can be back-calculated. The materials which were chosen are given in Table 2 together with their CTE [40]. The CTE was assumed to be constant for steel, aluminium and invar in the tested temperature range; in addition, for steel the linear CTE was measured on the same sample with a procedure explained in Section 4. Also deionised water, enclosed in a condom in

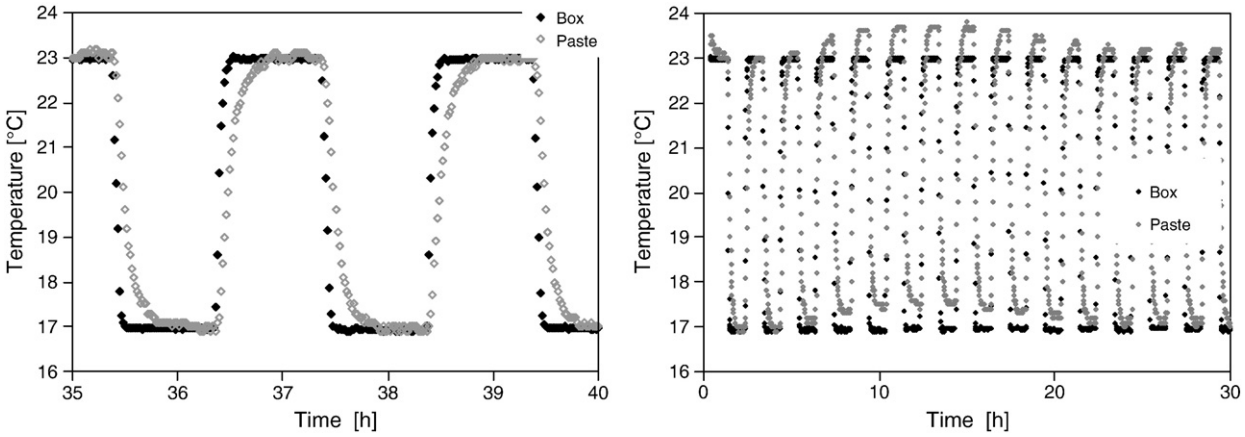

Fig. 4. Left: temperature profile in the perforated box and in a cement paste sample due to a temperature change in the bath from 23 °C to 17 °C and back every 60 min. Right: same type of graph as to the left, showing in addition the small temperature increase in the sample due to hydration heat.

the manner described above for the paste, was measured. Since temperature-dependent volume change of water is well known but not linear, the volume of water at the different temperatures was calculated according to [40].

The temperature-dependent density of the silicone oil measured with different materials is plotted in Fig. 7. A very similar curve for the temperature-dependent density of the oil is determined with carbon steel, aluminium and invar. For water, the density is slightly higher, which can be attributed to the uncertainties introduced by the presence of the condom and of the metallic clamp. The density of the oil is generally lower than the average values given by the oil producer. However, the determined density change of the oil as a function of temperature is very similar for all materials and even similar to the specification of the oil producer. For the following calculation of the volume of the cement paste, the average linear fit of temperature-dependent density change determined by carbon steel, aluminium and invar is used (Eq. (5)).

$$\rho_L(T) = 0.957796 - 0.00092202 \cdot T \tag{5}$$

To increase the accuracy in the determination of the temperature-dependent volume of the cement paste, the condom and the clamp have to be taken into account; the string to which the sample is suspended is neglected since most of it is above the oil level. The average mass of the remaining piece of the condom was 0.39 g. This was determined by weighing the whole condom and the piece that was cut off after closing the sample with the clamp on several samples. The clamp is industrially produced and has a constant weight of 0.69 g. The volume at 20 °C was determined by weighing several condoms or clamps in the air and under water. The volumetric CTE was assumed to be $600 \cdot 10^{-6}$/°C for the condom and $69 \cdot 10^{-6}$/°C for the clamp.

3.6. Data analysis

The volume change of the cement paste only, calculated from the mass plot in Fig. 5, is shown in Fig. 8. The few points which are furthest from the general curve at the beginning of every temperature step are due to the fact that recording of temperature and mass cannot be started exactly at the same time. When the temperature starts to change very quickly at the beginning of the temperature step, the mass is recorded with a delay of about 15 s which leads to an inaccurate determination of the paste volume. However, since these points are not taken into account for the following calculation, no correction is needed.

The volume change due to the temperature variation is superimposed to the volume change due to autogenous shrinkage, which has a significant impact on the total deformation especially in the first 8–10 h. Moreover, the volume change is delayed due to delayed temperature change in the sample compared to the buoyancy liquid. For these reasons, the CTE cannot simply be calculated from the volume step at an individual time.

To solve this problem, the encasing envelopes at 23 °C and at 17 °C, respectively, have been approximated by means of cubic smoothing splines [43]. For both, the lower and the upper envelopes separately, a

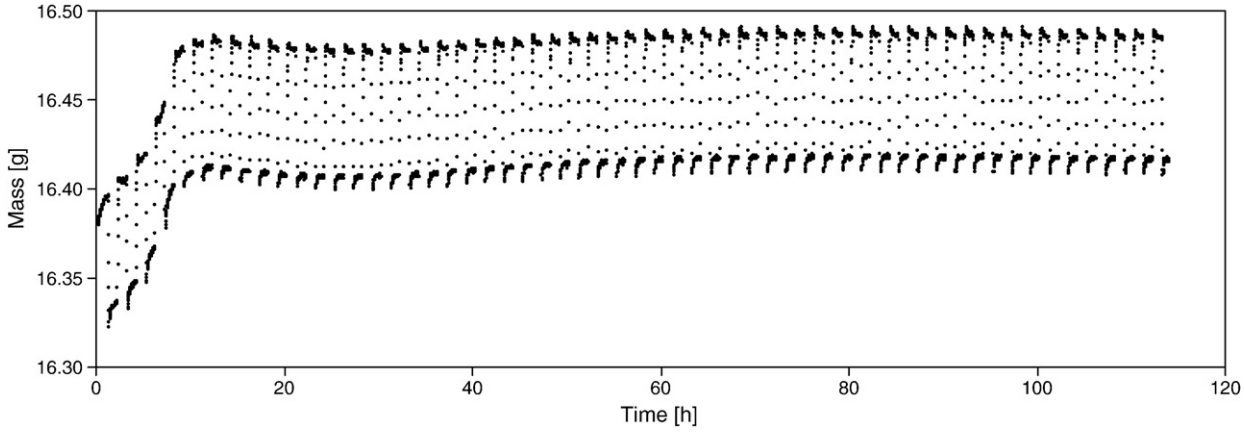

Fig. 5. Plot of the measured immersed mass of a cement paste subjected to a temperature change from 23 °C to 17 °C and back every 60 min.

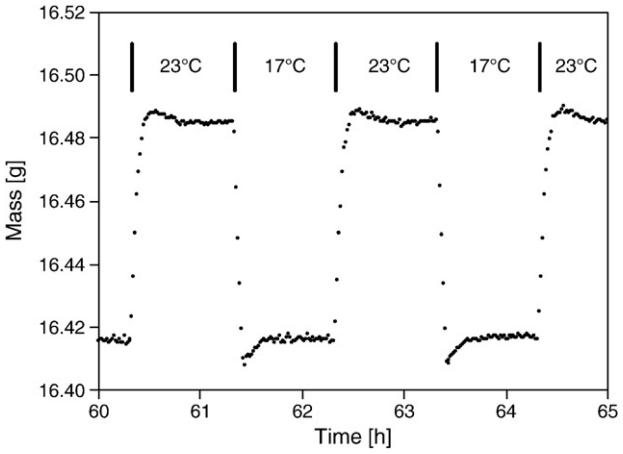

Fig. 6. Detail from Fig. 5 between 60 and 65 h. The mass is recorded every minute.

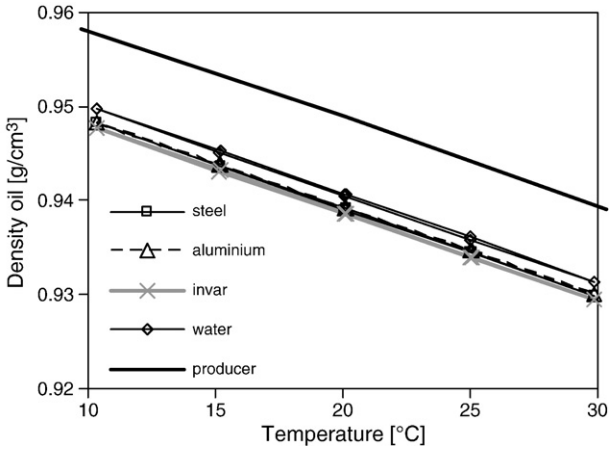

Fig. 7. Temperature-dependent density change of the buoyancy liquid (silicone oil) determined based on comparison with different materials and from the specification of the oil producer.

predefined amount of the measured volumetric values was being considered backwards, while starting with the last sample of each temperature step. This yields packages of measured data values at repetitive time intervals as the basis for the smoothing splines. The smoothing skills are useful for reducing the scattering noise and for ironing the periodic gaps between each two data packages; these gaps are quite large due to the splitting of the measured data into an upper and a lower data set, see Fig. 10. Thereby, a smoothing parameter $p \in [0,1]$ allows an appropriate interpolant between a straight line (at $p=0$), and a cubic spline (at $p=1$). The software has been written in Matlab command language. It returns two volumetric values at every defined time step, for the upper and for the lower temperature, respectively. The smoothed splines which have been derived from the plot in Fig. 8 are displayed in Fig. 9, while in Fig. 10, a detail of Fig. 9 in the first 15 h is shown.

Usually, in the range between 7 and 10 h where the volume change decreases rapidly due to autogenous shrinkage, the progress of the fitted spline is not reliable, owing to the inevitable gaps between the data packages (see above). As soon as the rapid decrease due to autogenous shrinkage is overlapped by a temperature change, those gaps inhibit accurate interpolation. The accuracy of the interpolation in this range is moreover strongly dependent on the smoothing factor. With decreasing smoothing factor, the accuracy of the interpolation is decreasing as well while, at the same time, the scatter of the calculated CTE in time over the whole time range is decreasing. Considering this relation, a constant smoothing factor of 0.6 was chosen for fitting all curves belonging to cement paste. Under these conditions, the square of the mean square error of the single points which are taken into account for fitting in the range between 14 and 112 h for the sample in Fig. 9 corresponds to 9.2–18.9% of the volume gap between the upper and the lower fitted curve. However, when the square of the mean square error of the data packages from the fit is calculated, it is only 1.6–3.2% of the volume gap. Similar errors were calculated for repeated test samples.

Table 2
Coefficient of volumetric thermal expansion (β_T) at 20 °C of the materials used to determine temperature-dependent density change of the buoyancy liquid.

Material [–]	Vol CTE 10e−6/°C
Carbon steel	33
Aluminium	71
Invar	3.6
Water	207

4. Results and discussion

From the resulting interpolated volume characteristics, the time-dependent CTE can be calculated according to Eqs. (3) and (4). The results for the cement paste sample object of the previous figures are shown in Fig. 11. The reproducibility of the procedure has been tested by two further identically produced and measured samples of the same cement paste (see Fig. 11).

In addition, volumetric measurements were compared to linear measurements of the CTE. Two cement paste samples with dimensions of $15 \times 15 \times 165$ mm^3 were prepared in a mould, covered with a glass plate and stored at 95% RH for 20 h. Afterwards, the specimens were sealed with aluminium foil and a plug gauge was glued on each end. Starting from the age of 24 h, the specimens were stored in silicone oil periodically either at 15 °C or at 25 °C for 1 h. The age-dependent CTE could then be calculated from the measured length at a specific temperature as the average of the two specimens (Fig. 11).

Between 13 and 90 h, the standard deviation of the three volumetric measurements is 1.08 µm/m/°C which corresponds to 4.3–7.2% of the total CTE. In the first few hours before final setting, a particularly high value for α_T has been measured, which rapidly decreases between 7 and 13 h. During this period, the scattering of the measured data points is larger than before or after. This is a direct consequence of the missing samples during interpolation due to the gaps combined with the sudden decrease of volume change (Fig. 10).

The correlation between linear und volumetric measurement is generally satisfactory, as the development in time of the CTE determined by the linear method display the same characteristic as the volumetric results. However, the linear points are generally about 3 µm/m/°C lower compared to the corresponding mean value of the three volumetric measurements. The reason for this difference was not investigated in detail in this study. Some factors that could influence the measurements are the presence of condom, clamp and string in the volumetric measurement, the different storage of the samples until the age of 24 h and the thermal dilation of the plug gauge and the glue in case of the linear measurement.

The noise in the measuring points within the CTE curve depends on the temperature difference within the temperature steps and on the length of the intervals. The influence of these variables was tested on cement paste samples (Fig. 12). While the increase of the temperature step from 6 to 8 °C (CP_60_8) and the change of the cycle duration from 60 min to 90 min (CP_90_8) have little effect on α_T, a decrease of the temperature step from 6 to 3 °C (CP_60_3) leads to a considerable increase of the noise. Accordingly, all the following tests were performed with a cycle duration of 60 min and a temperature step of 6 °C (23 °C/17 °C).

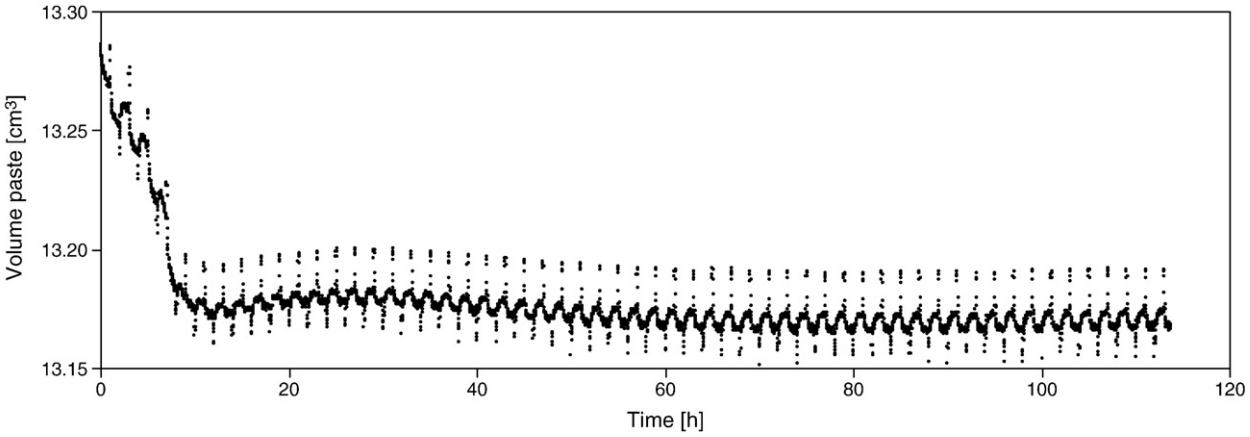

Fig. 8. Calculated time- and temperature-dependent volume of the cement paste.

To assess the results of α_T determined with silicone oil as buoyancy liquid, two additional measurements have been performed on cement paste immersed in deionised water. The temperature-dependent density change of pure water, $\rho_w(T)$, can be calculated according to Eq. (6) [44].

$$r_w(T) = 1000\left(1-(T+288.9414)/(508929.2\cdot(T+68.12963))\cdot(T-3.9863)^2\right) \quad (6)$$

The results of the thermal dilation coefficient measurement in a water bath are plotted in Fig. 13 together with an example of α_T determined with silicone oil as buoyancy liquid. As there was a problem in mass reading for the sample CP_water between 27 and 44 h, results are missing for this period. The linear CTE α_T determined in water shows a similar behavior to the one determined in silicone oil, which confirms the validity of the volumetric technique and the precision in the determination of the density changes of the silicone oil. In particular, in the fresh state there is a considerable scatter in α_T measured in a water bath, but the drop occurs at the same time and is in the same range as for silicone oil. There is also a following increase of α_T from about 12 to about 26 µm/m/°C for both samples. However, the oscillations within a single measurement are increased when water is used as buoyancy liquid. The increased uncertainty observed for measurements in water appears to be due to vibrations of the suspended sample that result in high-amplitude oscillations in the mass readings. These oscillations are much smaller when the samples are immersed in a silicone oil bath, supposedly as a result of the higher viscosity of the silicone oil compared to water. As a result, the choice for silicone oil as buoyancy liquid increases the stability and repeatability of the measurement.

Moreover, the absorption of water through the condom [33] has a considerable impact on the total strain. In the sample measured in water, the baseline onto which the temperature cycles are superimposed shows an apparent higher strain rate starting at about 10 h (Fig. 14, CP_water2_cycle). This higher strain rate can be attributed to absorption of water through the condom, which can be revealed by weighing the sample before and after the measurement. The sample submerged in water was weighed in air after the end of the measurement, showing a mass gain of about 80 mg. On the contrary, samples submerged in oil showed a slight decrease in mass when weighed in air after the measurement, on average 9.5 mg. Therefore, an additional influence of the permeability of the condom on the CTE cannot be excluded when the buoyancy fluid is water. It is worthwhile to repeat here that measuring the mass of the sample in air before and after the measurements allows identifying and eliminating samples in which large mass changes (due to absorption of fluid from the bath or due to drying) have occurred [33,45].

The autogenous strain determined in isothermal conditions at 20 °C (Fig. 14, CP_oil_iso) is very similar to the strain determined with temperature cycling between 23 °C and 17 °C (Fig. 14, CP_oil_cycle).

The proposed measuring technique might not only be applied to cement paste, but also to other hardening materials or to fluids. To validate the applicability and the sensitivity of the measuring method, the α_T of deionised water enclosed in a condom, of a non-hardening paste of limestone powder mixed with water, as well as of a cement

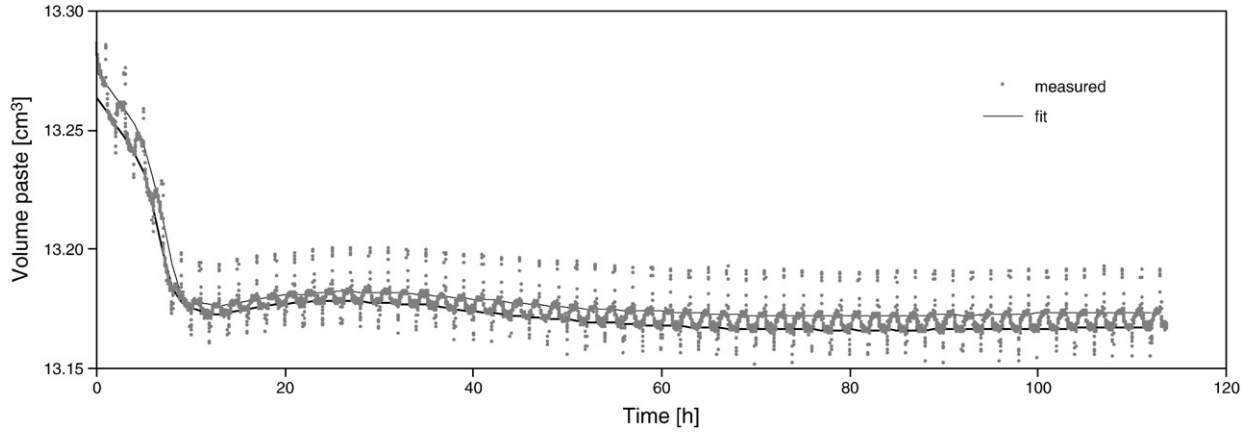

Fig. 9. Calculated time- and temperature-dependent volume of the cement paste and curve fit for 23 °C and 17 °C.

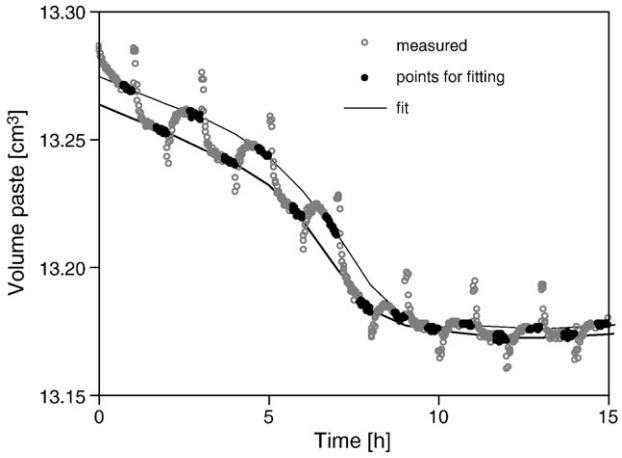

Fig. 10. Detail of Fig. 9 for the first 15 h including measured volume of paste, points which are taken into account for curve fitting and fitted curves.

mortar with 41% by volume of sand with low water absorption and maximum grain size of 1 mm have additionally been measured (Fig. 15).

The non-hardening materials (water and limestone powder paste) exhibit a constant CTE over time. Linear CTE α_T at 20 °C of deionised water is determined as 67.5 µm/m/°C in average, which is only 2% lower than the value found in the literature, 69 µm/m/°C [40]. This difference is primarily supposed to be a result of the uncertainty in temperature-dependent density change of the silicone oil and of the influence of the condom and the clamp. The α_T of the LP paste is lower than the one of pure water, which seems to be reasonable when comparing with the α_T of the components. Assuming a α_T of 69 µm/m/°C for deionised water and 5 µm/m/°C [46] at 20 °C for limestone (density 2.76 g/cm^3), α_T of the paste is calculated to be 34 µm/m/°C. The average α_T measured with the volumetric method is 32 µm/m/°C and therefore 6% lower than the calculated value.

A considerable difference in CTE is observed between mortar and cement paste. First, there is a difference in the very first hours: while the α_T of cement paste is lower and increases with time, the α_T of mortar starts with higher values and drops constantly. The drop of α_T occurs at roughly the same time for mortar and cement paste and stops at a minimum value of about 12 µm/m/°C for the cement paste and 10 µm/m/°C for the mortar. The subsequent increase of α_T in time is higher for the cement paste, which reaches values of about 26 µm/m/°C after 5 days. In the mortar, the α_T increases gradually up to about 16 µm/m/°C at the end of the experiment (about 90 h).

According to the results presented above, the reproducibility of the method proves to be sufficient to perform investigations of the time-dependent CTE behavior of different cementitious materials. The tested cement paste shows an increase of the CTE in the very first hours after mixing. The fast drop of CTE after about 7 h coincides with final setting measured by Vicat needle and is a consequence of the solidification of the paste. Interestingly, final setting is also the time when deviation of chemical and autogenous shrinkage and intense acoustic activity are measured in cement pastes [47,48].

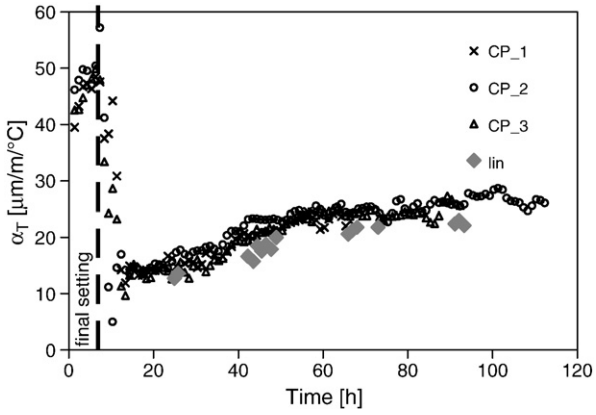

Fig. 11. Time-dependent linear CTE α_T of three identical cement pastes measured by the volumetric method with temperature steps of 23–17 °C every 60 min (CP_1, CP_2 and CP_3). Additionally, some points measured with a linear method are also shown (lin).

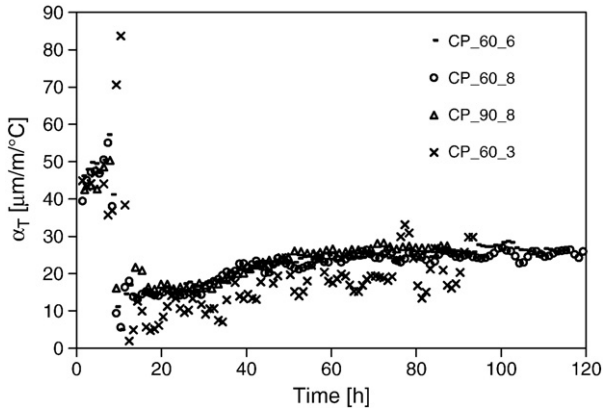

Fig. 12. Effect of cycle duration and temperature step on the results of time-dependent α_T. Notation: CP_duration(min)_temperaturestep(°C).

Once the cement paste solidifies, the CTE suddenly drops and seems not to be significantly affected by the formation of further hydration products, which form in the following hours. The linear increase of CTE from about 12 to 26 µm/m/°C, which starts after about 30 h, can be explained by the self-desiccation of the low w/c paste. As the relative humidity decreases in the cement paste, the CTE increases [17,18].

The lower CTE of the mortar can be explained by the presence of 41% by volume of sand, which has lower CTE than the cement paste and high stiffness. The sand acts therefore as an internal restraint to the thermal deformations of the cement paste and limits the total thermal dilation of the mortar.

5. Conclusions and outlook

The proposed volumetric method allows studies of the development in time of the CTE in hardening materials. The method proves to have a good repeatability. The accuracy of the measurements was investigated at temperature cycles of different amplitudes, and the temperature regime was optimized accordingly. A crucial aspect of the method was the precise and fast temperature conditioning of the sample, together with the accurate determination of the density of the buoyancy oil.

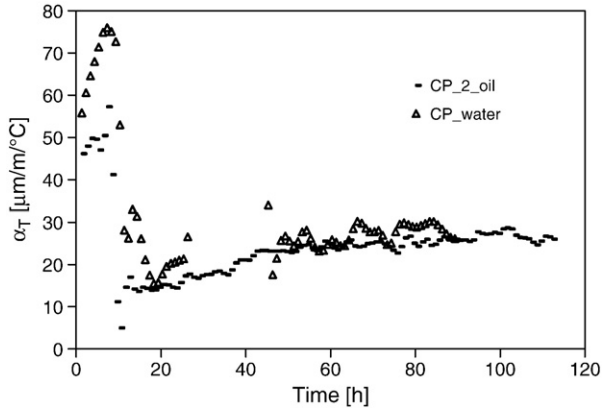

Fig. 13. α_T determined with either silicone oil or deionised water as buoyancy liquid.

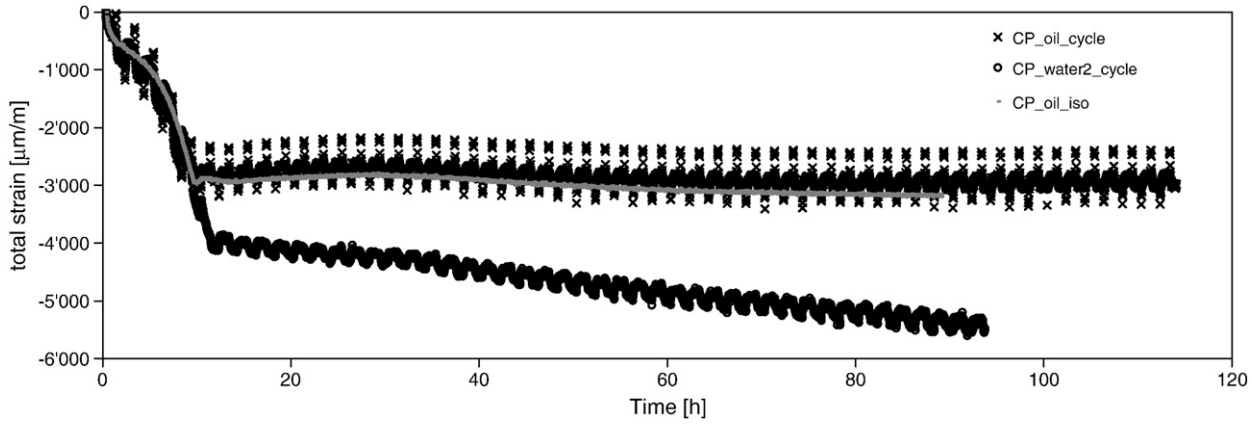

Fig. 14. Total strain determined with either silicone oil or deionised water as buoyancy liquid and temperature cycling (CP_oil_cycle, CP_water2_cycle). The graph shows also an isothermal measurement in silicone oil at 20 °C (CP_oil_iso).

An increase of CTE in the very first hours after mixing was measured for cement pastes with w/c 0.3. The fast drop of CTE after about 7 h coincides with setting, while the subsequent increase over several days can be attributed to self-desiccation of the paste. An increase of CTE after setting time is also observed in mortars, however the effect of self-desiccation is not as pronounced as for cement pastes. The CTE of an inert mixture of limestone powder and water matched well with the calculated values.

In a follow up study, the effect on the CTE of cement pastes and mortars of different supplementary cementitious materials and admixtures will be examined. The effect of admixtures which are able to influence the self-desiccation of the cement paste (i.e., shrinkage-reducing admixtures and superabsorbent polymers) is of particular interest. Furthermore, possible applications of the method for studies on different types of mineral and non-mineral binders can be envisaged, for instance calcium aluminate and calcium sulfoaluminate cements and thermoplastics.

Acknowledgements

Useful discussion with Jason Weiss, Gaurav Sant and Andreas Leemann is gratefully acknowledged. The authors thank Walter Trindler and Carmelo Di Bella for their help with the experimental setup.

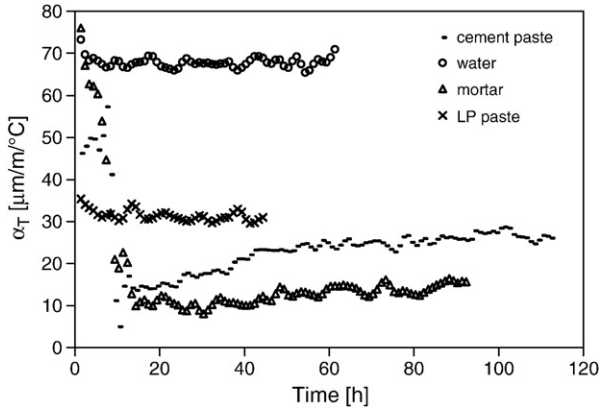

Fig. 15. Time-dependent linear CTE α_T of different materials. Temperature cycles 23 °C/17 °C every 60 min. LP paste = limestone powder paste.

References

[1] J. Bisschop, J.G.M. van Mier, Effect of aggregates on drying shrinkage microcracking in cement-based composites, Mater. Struct. 35 (8) (2002) 453–461.
[2] P. Lura, O.M. Jensen, J. Weiss, Cracking in cement paste induced by autogenous shrinkage, Mater. Struct. 42 (8) (2009) 1089–1099.
[3] M. Pigeon, G. Toma, A. Delagrave, B. Bissonette, J. Marchand, J.C. Prince, Equipment for the analysis of the behaviour of concrete under restrained shrinkage at early ages, Mag. Concr. Res. 52 (4) (2000) 297–302.
[4] S. Igarashi, A. Bentur, K. Kovler, Autogenous shrinkage and induced restraining stresses in high-strength concretes, Cem. Concr. Res. 30 (11) (2000) 1701–1707.
[5] P. Lura, K. van Breugel, I. Maruyama, Effect of curing temperature and type of cement on early-age shrinkage of high-performance concrete, Cem. Concr. Res. 31 (12) (2001) 1867–1872.
[6] R. Loser, A. Leemann, Shrinkage and restrained shrinkage cracking of self-compacting concrete compared to conventionally vibrated concrete, Mater. Struct. 42 (1) (2009) 71–82.
[7] S. Lepage, M. Baalbaki, E. Dallaire, P.-C. Aïtcin, Early shrinkage development in a high performance concrete, Cem. Concr. Agg. 21 (1999) 31–35.
[8] K. Kovler, Shock of evaporative cooling of concrete in hot dry climates, Concr. Int. 17 (10) (1995) 65–69.
[9] Ø. Bjøntegaard, E.J. Sellevold, Interaction between thermal dilation and autogenous deformation in high performance concrete, Mater. Struct. 34 (2001) 266–272.
[10] M. Viviani, B. Glisic, I.F.C. Smith, System for monitoring the evolution of the thermal expansion coefficient and autogenous deformation of hardening materials, Smart Mater. Struct. 15 (2006) N137–N146.
[11] M. Viviani, B. Glisic, I.F.C. Smith, Separation of thermal and autogenous deformation at varying temperatures using optical fiber sensors, Cem. Concr. Comp. 29 (6) (2007) 435–447.
[12] A. Kamen, E. Denarié, H. Sadouki, E. Brühwiler, Thermo-mechanical response of UHPFRC at early age—experimental study and numerical simulation, Cem. Concr. Res. 38 (6) (2008) 822–831.
[13] G. De Schutter, Finite element simulation of thermal cracking in massive hardening concrete elements using degree of hydration based material laws, Comput. Struct. 80 (27–30) (2002) 2035–2042.
[14] R. Faria, M. Azenha, J.A. Figueiras, Modelling of concrete at early ages: application to an externally restrained slab, Cem. Concr. Comp. 28 (6) (2006) 572–585.
[15] Z.P. Bažant, J.-K. Kim, L. Panula, Improved prediction model for time-dependent deformations of concrete: part 1—shrinkage, Mater. Struct. 24 (1991) 327–345.
[16] O.M. Jensen, P.F. Hansen, Influence of temperature on autogenous deformation and relative humidity change in hardening cement paste, Cem. Concr. Res. 29 (4) (1999) 567–575.
[17] E.J. Sellevold, Ø. Bjøntegaard, Coefficient of thermal expansion of cement paste and concrete: mechanisms of moisture interaction, Mater. Struct. 39 (2006) 809–815.
[18] Z.C. Grasley, D.A. Lange, Thermal dilation and internal relative humidity of hardened cement paste, Mater. Struct. 40 (2007) 311–317.
[19] H. Ai, J.F. Young, G.W. Scherer, Thermal Expansion Kinetics: method to measure permeability of cementitious materials: II, application to hardened cement pastes, J. Am. Ceram. Soc. 84 (2) (2001) 385–391.
[20] C. Boulay, Determination of coefficient of thermal expansion, in: A. Bentur (Ed.), Early Age Cracking in Cementitious Systems, State-of-the-Art Report Number 25, RILEM TC 181, RILEM, 2003, pp. 217–224.
[21] G. De Schutter, Thermal properties, in: A. Bentur (Ed.), Early Age Cracking in Cementitious Systems, State-of-the-Art Report Number 25, RILEM TC 181, RILEM, 2003, pp. 121–125.
[22] M. Sarkis, J.L. Granju, M. Arnaud, G. Escadeillas, Coefficient de dilatation thermique d'un mortier frais, Mater. Struct. 35 (2002) 415–420.
[23] D. Cusson, T. Hoogeveen, Measuring early-age coefficient of thermal expansion in high-performance concrete, in: Lura Jensen, Kovler (Eds.), RILEM Int. Conf. Volume

Changes of Hardening Concrete, 20–23 August 2006 (Lyngby, Denmark), 2006, pp. 321–330.
[24] I. Shimasaki, K. Rokugo, H. Morimoto, Thermal expansion coefficient of concrete at very early ages, in: Mihashi, Wittmann (Eds.), Proc. Int. Workshop Sendai, Japan, August 2000. Control of Cracking in Early Age Concrete, Swets & Zeitlinger, Lisse, 2002, pp. 29–36.
[25] M. Ozawa, H. Morimoto, Estimation method for thermal expansion coefficient of concrete at early ages, in: Lura Jensen, Kovler (Eds.), RILEM Int. Conf. Volume Changes of Hardening Concrete, 20–23 August 2006 (Lyngby, Denmark), 2006, pp. 331–339.
[26] P. Laplante, C. Boulay, Evolution du coéfficient de dilatation thermique du béton en fonction de sa maturité aux tout premiers âges, Mater. Struct. 27 (1994) 596–605.
[27] H. Kada, M. Lachemi, N. Petrov, O. Bonneau, P.-C. Aïtcin, Determination of the coefficient of thermal expansion of high performance concrete from initial setting, Mater. Struct. 35 (2002) 35–41.
[28] C. Boulay, C. Patiès, Mesure des déformations du béton au jeune âge, Mater. Struct. 26 (1993) 308–314.
[29] D. Cusson, T. Hoogeveen, New test method for determining coefficient of thermal expansion at early age in high-performance concrete, 12th Int. Conf. on Chemistry of Cement, Montreal, Canada, July 2007, 2007 12 pp.
[30] A. Loukili, A. Chopin, A. Khelidj, J.-Y. Le Touzo, A new approach to determine autogenous shrinkage of mortar at an early age considering temperature history, Cem. Concr. Res. 30 (2000) 915–922.
[31] P. Turcry, A. Loukili, L. Barcelo, J.M. Casabonne, Can the maturity concept be used to separate the autogenous shrinkage and thermal deformation of a cement paste at early age? Cem. Concr. Res. 32 (2002) 1443–1450.
[32] P. Lura, O.M. Jensen, A discussion of the paper: 'On the measurement of free deformation of early age cement paste and concrete' by Ø. Bjøntegaard, T. A. Hammer and E. J. Sellevold, Cem. Concr. Comp. 27 (7–8) (2005) 854–856.
[33] P. Lura, O.M. Jensen, Measuring techniques for autogenous strain of cement paste, Mat. Struct. 40 (2007) 431–440.
[34] G. Sant, P. Lura, W.J. Weiss, Measurement of volume change in cementitious materials at earle ages: review of testing protocols and interpretation of results, Transp. Res. Board Rec. 1979 (2006) 21–29.
[35] T. Koufopoulos, P.S. Theocaris, Shrinkage stresses in two-phase materials, J. Comp. Mat. 3 (1969) 308–320.
[36] A.W. Snow, J.P. Armistead, A simple dilatometer for thermoset cure shrinkage and thermal expansion measurements, J. Appl. Polym. Sci. 52 (3) (1994) 401–411.
[37] M. Shimbo, M. Ochi, Y. Shigeta, Shrinkage and internal stress during curing of epoxide resins, J. Appl. Polym. Sci. 26 (7) (1981) 2265–2277.
[38] Z. Yan, S. Sidhu, T. Carrick, J. McCabe, Response to thermal stimuli of glass ionomer cements, Dent. Mater. 23 (5) (2007) 597–600.
[39] Lauda Ecoline factsheet, 2009.
[40] CRC Handbook of Chemistry and Physics, 67th EditionCRC Press, 1986-1987 F-4–F-5.
[41] S.L. Meyers, Thermal expansion characteristics of hardened cement paste and of concrete, Highway Res. Board Proc. 30 (1950) 193–203.
[42] R.A. Helmuth, Dimensional changes of hardened Portland cement pastes caused by temperature changes, Highway Res. Board Proc. 40 (1961) 315–336.
[43] C.S. Duris, Algorithm 547: Fortran routines for discrete cubic spline interpolation and smoothing, ACM Trans. Math. Softw. 6 (1) (1980) 92–103.
[44] S.C. McCutcheon, J.L. Martin, T.O. Barnwell, Water quality, in: D.R. Maidment (Ed.), Handbook of Hydrology, McGraw-Hill, New York, 1993, Chapter 11.
[45] P. Lura, J. Weiss, A discussion of the paper: "Free autogenous strain of early-age cement paste: metrological development and critical analysis" by M. Bouasker, P. Mounanga, A. Khelidj and R. Coué, Adv. Cement Res. 22 (1) (2010) 59–60.
[46] P.R. Dickinson, N. Thornton, Cracking and Building Movement, RICS Business Services Limited, Conventry, UK, 2004 pp. 175.
[47] P. Lura, J. Couch, O.M. Jensen, J. Weiss, Early-age acoustic emission measurements in hydrating cement paste: evidence for cavitation during solidification due to self-desiccation, Cem. Concr. Res. 39 (10) (2009) 861–867.
[48] G. Sant, M. Dehadrai, D. Bentz, P. Lura, C.F. Ferraris, J.W. Bullard, J. Weiss, Detecting the fluid–solid transition in cement paste, Concr. Int. 31 (6) (2009) 54–58.